Curcumin encapsulated polylactic acid nanoparticles embedded in alginate/ gelatin bioinks for in situ immunoregulation: Characterization and biological assessment

International Journal of Biological Macromolecules 221 (2022) 1218–1227

Contents lists available at ScienceDirect

International Journal of Biological Macromolecules

journal homepage: www.elsevier.com/locate/ijbiomac

Curcumin encapsulated polylactic acid nanoparticles embedded in alginate/gelatin bioinks for *in situ* immunoregulation: Characterization and biological assessment

Fernanda Zamboni [a,b], Guang Ren [a], Mario Culebras [c], John O'Driscoll [e], Jack O'Dwyer [e], Elizabeth J. Ryan [b,f], Maurice N. Collins [a,b,d,*]

[a] *Bernal Institute, University of Limerick, Ireland*
[b] *Health Research Institute, University of Limerick, Ireland*
[c] *Institute of Material Science, University of Valencia, Spain*
[d] *SFI AMBER, University of Limerick, Ireland*
[e] *School of Engineering, University of Limerick, Ireland*
[f] *Department of Biological Sciences, University of Limerick, Ireland*

A R T I C L E I N F O

Keywords:
Curcumin
Nanoparticles
Alginate
Hydrogel
Bioink
Immunomodulation
Intervertebral disc degeneration

A B S T R A C T

Curcumin is a known naturally occurring anti-inflammatory agent derived from turmeric, and it is commonly used as a herbal food supplement. Here, in order to overcome the inherent hydrophobicity of curcumin (Cur), polylactic acid (PLA) nanoparticles (NPs) were synthesised using a solvent evaporation, and an oil-in-water emulsion method used to encapsulate curcumin. Polymeric NPs also offer the ability to control rate of drug release. The newly synthesised NPs were analysed using a scanning electron microscope (SEM), where results show the NPs range from 50 to 250 nm. NPs containing graded amounts of curcumin (0 %, 0.5 %, and 2 %) were added to cultures of NIH3T3 fibroblast cells for cytotoxicity evaluation using the Alamar Blue assay. Then, the curcumin NPs were incorporated into an alginate/gelatin solution, prior to crosslinking using a calcium chloride solution (200 nM). These hydrogels were then characterised with respect to their chemical, mechanical and rheological properties. Following hydrogel optimization, hydrogels loaded with NP containing 2 % curcumin were selected as a candidate as a bioink for three-dimensional (3D) printing. The biological assessment for these bioinks/hydrogels were conducted using THP-1 cells, a human monocytic cell line. Cell viability and immunomodulation were evaluated using lactate dehydrogenase (LHD) and a tumour necrosis factor alpha (TNF-α) enzyme-linked immunosorbent (ELISA) assay, respectively. Results show that the hydrogels were cytocompatible and supressed the production of TNF-α. These bioactive hydrogels are printable, supress immune cell activation and inflammation showing immense potential for the fabrication of tissue engineering constructs.

1. Introduction

Low back pain (LBP) affects over 600 million individuals worldwide, being considered one of the top global causes of disability-adjusted life years [1]. LBP also carries a huge negative healthcare burden, exceeding over $100 billion/year in the USA alone [2]. Although the aetiology of LBP is multifactorial, intervertebral disc (IVD) degeneration (IVDD) is regarded as a major contributor to this pathology. In IVDD, progressive destruction of the extracellular matrix (ECM) caused by overexpression of matrix metalloproteases (MMP), enhanced senescence, disc cell death, inflammation, and impairment of tissue biomechanical function are observed in result of environmental and genetic factors. The inflammatory process, driven by the pro-inflammatory cytokines, interleukin- (IL-) 1β and tumour necrosis factor-α (TNF-α) underpins the pathogenesis of IVDD and LBP [3]. Chronic LBP due to IVDD is generally treated by the administration of systemic anti-inflammatory agents and physiotherapy [4]. However, patients that are unable to obtain relief from conservative therapies are considered for surgical treatments including discectomy to remove herniated discs, spinal fusion surgery used to connect two vertebrae to limit the movement of the spinal motion segment [5]. Other treatments strategies include, cell-based therapy and artificial disc replacements designed to restore and maintain the

* Corresponding author at: Health Research Institute, University of Limerick, Ireland.
E-mail address: Maurice.collins@ul.ie (M.N. Collins).

https://doi.org/10.1016/j.ijbiomac.2022.09.014
Received 8 May 2022; Received in revised form 2 September 2022; Accepted 3 September 2022
Available online 7 September 2022

Table 1
Drying variables of Cur@PLA NPs.

Pressure	20 mTorr			
Time (minutes)	60	90	90	60
Temperature (°C)	−20	−5	5	20

spinal range of motion [6].

Therefore, the development of tissue engineering strategies combining various biomaterials, cells and other factors are needed to recreate a suitable matrix capable to restore the mechanical and biological properties of the IVD tissue [7]. *In vivo*, the IVD is the load-bearing structure of the spine and is subjected to spinal tension, torsion, compression, and bending. The IVD is an avascular structure being divided into three distinct anatomical parts. The inner part is called the nucleus pulposus, which contains a highly hydrated gel-like matrix comprising proteoglycans (PGs) and type II collagen which acts as a shock absorbent in order to resist compressive loading. An intermediate part called annulus fibrosus, consists of lamellae in which parallel type I collagen fibres are located and help the IVD maintain its integrity from bending, stretching, and twisting. The outer part of IVD is called end plate, which consist of osseous and two hyaline cartilages [8].

Curcumin has shown to protect chondrocytes from degenerative distress when under intermittent cyclic tension stimulation stress. Curcumin-mediated autophagy enhanced the adaptability of endplate chondrocytes to high-intensity tension load, thereby relieving intervertebral disc degeneration [9]. Moreover, curcumin has also shown to reduce senescence-associated secretory phenotype (SASP) factors of senescent IVD cells associated with inflammation and back pain. Following curcumin treatment, mRNA expression levels of SASP factors decreased by four to 32-fold compared to the untreated groups. Senescent cell clearance decreased, protein expression of matrix metalloproteases reduced, and proinflammatory cytokines levels of IL-1, IL-6 and IL-8 reduced. Overall, extracellular matrix content increased following treatment with curcumin, as validated by an increase in proteoglycan content in pellet cultures and surrounding culture media [10].

Curcumin is a yellow phytochemical compound derived from turmeric (*Curcuma longa* L) that belongs to the polyphenol family of diarylheptanoids [11]. Curcumin has been used for centuries as a bioactive ingredient for various medicinal preparations in traditional Chinese medicine and Ayurveda [12], showing safety even at high doses [13]. It has been used to treat common inflammatory diseases, biliary and liver disorders, rheumatism, and sinusitis amongst others [14]. Curcumin is a well-known natural anti-inflammatory agent that inhibits production of TNF-α and IL-1β and limits oxidative stress [15–17]. However, curcumin is a highly hydrophobic molecule, with low solubility in water which impairs bioavailability [12]. A variety of methods have been employed to enhance curcumin pharmacokinetic properties, including the encapsulation of curcumin in various nanocarriers such as the incorporation of curcumin in phospholipid complexes, liposomes, and polymeric NPs [14]. Polymeric NPs are advantageous because they offer increased absorption, controlled drug release, lengthened blood circulation and have good stability in the gastrointestinal tract [16].

The encapsulation of curcumin in PLA NPs (Cur@PLA NPs) and their incorporation in hydrogel networks may prove beneficial to the development of tissue engineered nucleus pulposus substitutes, as it can decrease the local inflammatory response associated with degenerative conditions.

The regeneration of nucleus pulposus tissues is very limited due to the change in cellular composition of nucleus pulposus during human development. Prior to adolescence, large vacuolated notochordal cells can be found in the nucleus pulposus, but they disappear with adolescence, being replaced by small nucleus pulposus cells, which diminish the regenerative capacity of the IVD [18].

Injectable biomaterials may be applicable to symptomatic early to moderate disc degeneration, while tissue engineered constructs may be used to partial or total disc replacement [18]. In this regard, to bridge the gap between the mechanical and biological requirements for nucleus pulposus replacement, this study proposes the use of alginate and gelatin to create a suitable hydrogel for IVD replacement. Alginate is a natural polymer containing 1,4-linkedD-mannuronic acid and L-guluronic acid units that can undergo ionic cross-linking with divalent cations that bind to the guluronate blocks [19]. However, due to the low cell adhesiveness

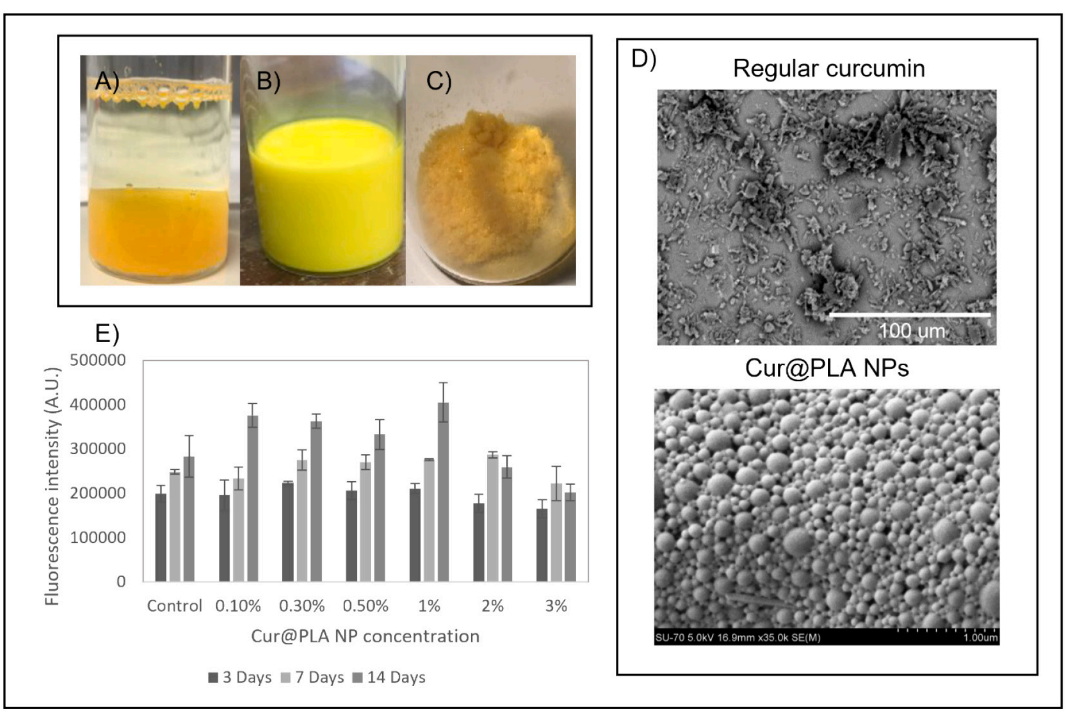

Fig. 1. Synthesis of Cur@PLA NPs. A) Organic phase (curcumin + PLA + DCM) with aqueous phase (water + SDS). B) Sonicated Emulsion. C) Freeze dried Cur@PLA NPs. D) SEM image of Cur@PLA NPs. E) Viability of NHI 3 T3 fibroblasts incubated with various concentrations of Cur@PLA NPs.

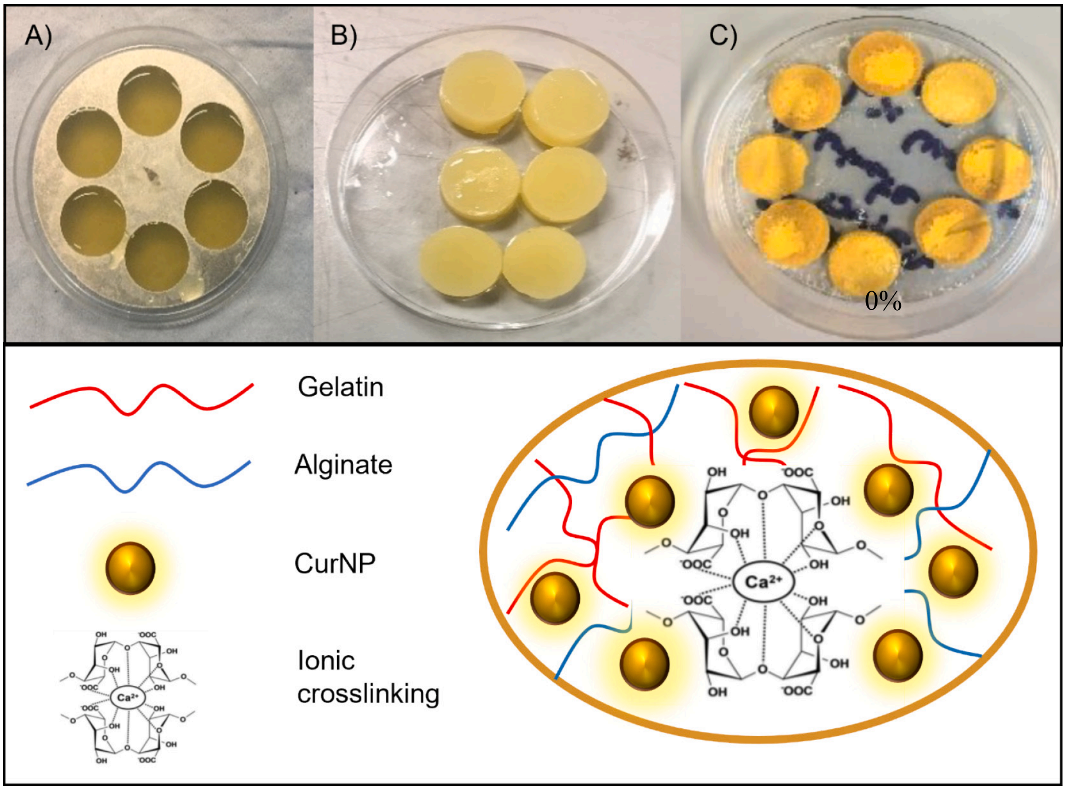

Fig. 2. Representative Cur@PLA NP-loaded alginate/gelatin hydrogels. A) Cylindrical mould casting of pre-crosslinked Cur@PLA NP-loaded alginate/gelatin solutions. B) Uniform, cylindrical hydrogels successfully cross-linked using $CaCl_2$. C) Hydrogels after freeze drying.

of alginate, the incorporation of gelatin, a hydrolysed form of collagen, will provide the domains for the tripeptide Arginine-Glycine-Aspartate (RGD), which is necessary to promote cell adherence in these hydrogels [20]. Gelatin hydrogels have been shown optimal nucleus pulposus cells proliferation at a concentration of 5 % [21]. The combination of alginate and gelatin has been shown to have a positive effect on cell growth and proliferation. The cell viability of normal human dermal fibroblasts in alginate gels and alginate-gelatin gels showed that cell viability significantly increased in alginate-gelatin gels than in alginate gels alone [22].

In this landscape, Cur@PLA NPs were synthesised using an oil in water, solvent evaporation method to overcome the poor bioavailability and hydrophobicity of regular curcumin. These Cur@PLA NPs were incorporated into a hydrogel (5 % alginate: 5 % gelatin wt%) and serial mechanical, physical, chemical and biological assessments were carried out to evaluate its suitability as a bioink for 3D printing of intravertebral disc substitutes where the curcumin is envisaged to be delivered locally to the nucleus pulposus to alleviate the inflammatory response observed in IVDD.

2. Materials and methods

2.1. Materials

Polylactic acid (Ingeo Biopolymer 3001D) with injection moulding grade (specific density = 1.24 and melting temperature = 200 °C) was supplied by Natureworks, Minnetonka. Alginate, gelatin and calcium chloride ($CaCl_2$) were purchased from BioBots Inc. (currently known as Allevi 3D Systems, Philadelphia, USA). Dichloromethane (DCM) was purchased from Lennox Laboratories (Dublin, Ireland). Enzyme-linked immunosorbent assay (ELISA) Max human tumour necrosis factor alpha (TNF-α) was purchased from Biolegend (San Diego, CA, USA). Curcumin powder, alamar blue (AB), lactate dehydrogenase (LDH) assay kit, Dulbecco's modified Eagle Medium (DMEM), Roswell Park Memorial Institute (RPMI) medium, trypsin-EDTA 0.25 %, foetal bovine serum (FBS), phosphate buffered saline (PBS), L-glutamine and antibiotics and all other reagents used in this work were of analytical grade purchased from Sigma Aldrich (St. Louis, MO, USA). NIH/3 T3 fibroblast cell line was obtained from the American Type Culture Collection (ATCC, USA). THP-1 cell line derived from human monocytes was purchased from commercial sources.

2.2. Encapsulation of curcumin in PLA nanoparticles (Cur@PLA NPs)

Cur@PLA NPs were produced using a solvent evaporation, oil in water emulsion procedure. Briefly, PLA (0.23 g) was dissolved in 5 mL of DCM. Once complete dissolution of PLA, curcumin (0.025 g) was added to the DCM/PLA solution and allowed to dissolve. In parallel, 0.01 g of sodium dodecyl sulphate (SDS) was dissolved in 9.5 mL of deionized water. The curcumin/DCM/PLA solution (oil phase) was added into the SDS/water solution (aqueous phase) and stirred for 15 min at 600 rpm at room temperature (RT). Then, the mixture was sonicated (Soniprep 150) for 3 min at an amplitude intensity of 8–9 μm. The mixture was left overnight under stirring inside a fume hood at RT to allow evaporation of DCM. Later, the mixture was heated to 50 °C to ensure DCM was fully evaporated. The remaining yellow-coloured solution containing the Cur@PLA NPs was filtered into a vial and stored in a fridge until further use.

2.3. Morphological characterization of Cur@PLA NPs

The Cur@PLA NP solution was freeze-dried using Virtis Advantage freeze dryer under the parameters shown in Table 1. Following the freeze-drying process, the Cur@PLA NPs were placed over a conductive copper tape and gold coated under 20 mA for 1 min in a vacuum chamber at a pressure of 1×10^{-1} Pa using a gold-sputter Emitech K550.

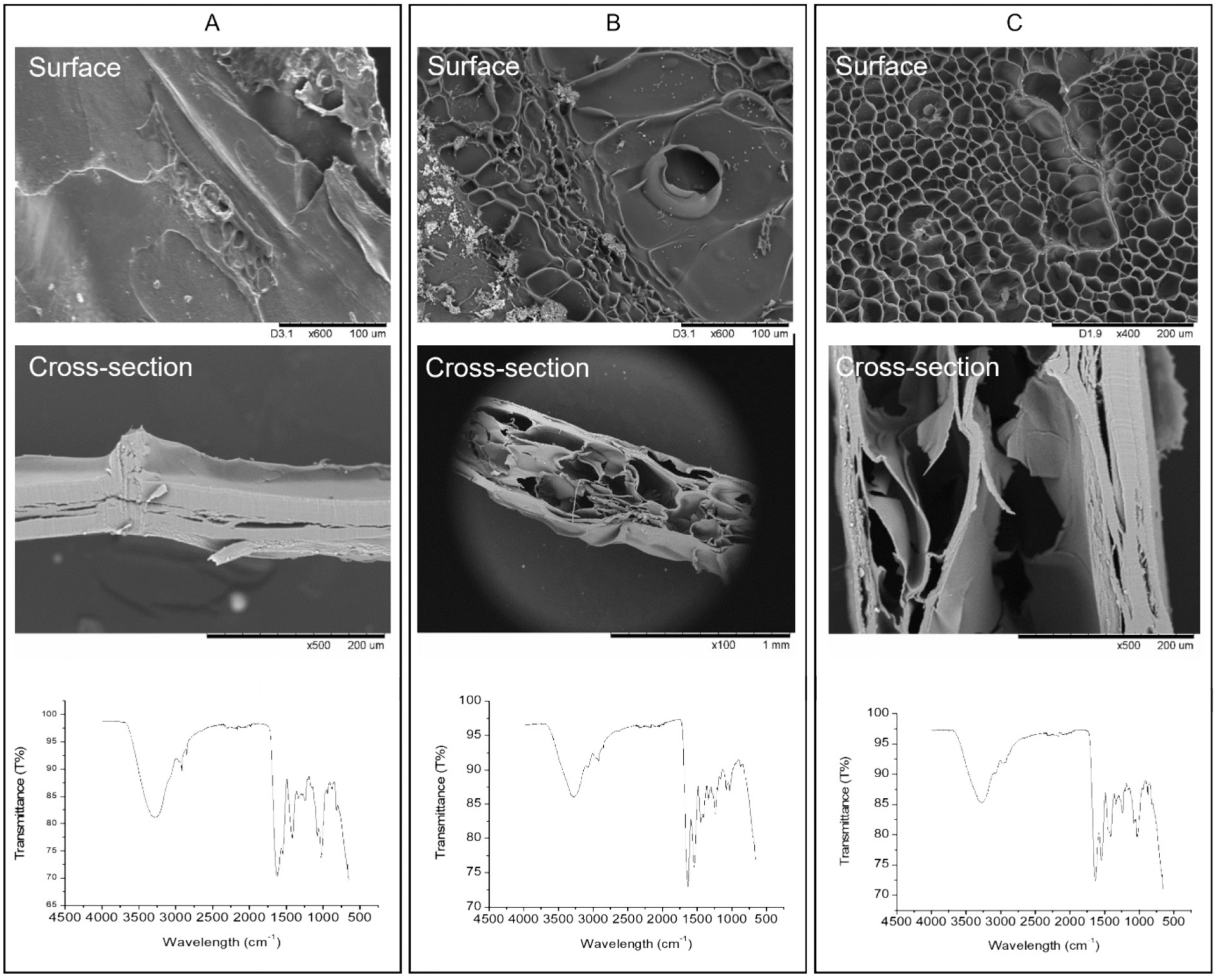

Fig. 3. Scanning electron micrographs of surface and cross-section areas of 0 % (A), 0.5 % (B) and 2 % (C) Cur@PLA NP-loaded alginate/gelatin hydrogels, accompanied with their respective FTIR spectra.

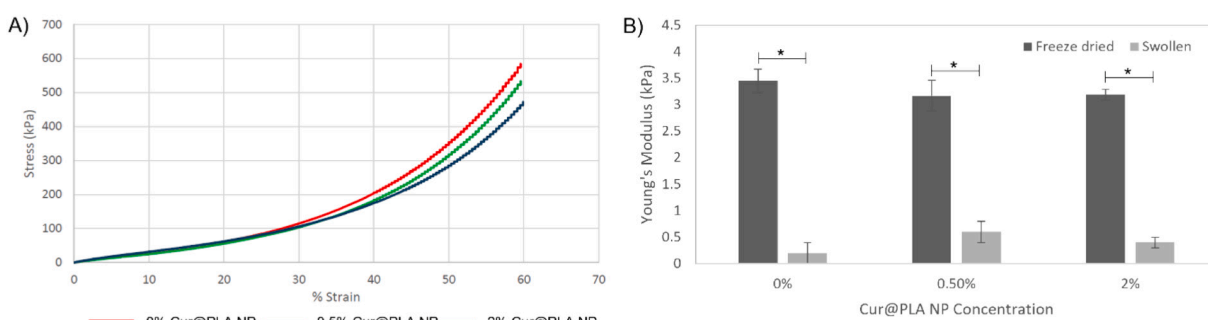

Fig. 4. Representative mechanical compression stress *vs.* strain curves of Cur@PLA NP-loaded alginate/gelatin hydrogels (A). Young's Moduli of freeze dried and swollen hydrogels (B).

The Cur@PLA NPs were finally analysed using a scanning electron microscope (SEM) Hitachi TM-1000 (Hitachi, Japan). Micrographs were used to evaluate the morphology of the Cur@PLA NPs and measure the size distribution using Image J software (National Institutes of Health, USA).

2.4. *In vitro cytocompatibility of Cur@PLA NPs*

Prior to all biocompatibility and immunomodulatory tests, Cur@PLA NPs solutions and Cur@PLA NP-loaded hydrogels were sterilized using an autoclave (Rodwell MP 24 Control) for 15 min at 120 °C.

NIH/3T3 cells were cultured in high glucose DMEM supplemented with glutamine, antibiotics (penicillin + streptomicyn) and 10 % FBS. Cells were maintained in the incubator at 37 °C in a humidified atmosphere with 5 % CO_2 until 80 % confluent. Cells were trypsinized and seeded (5×10^5 cells/mL) onto 24 well-plates pre-filled with various concentrations of Cur@PLA NPs/DMEM solutions (0 %, 0.1 %, 0.3 %, 0.5 %, 1 %, 2 %, and 3 % *w/v*). Cells were incubated for 3 days prior to the assessment of cell viability. Cell metabolic activity was analysed using resazurin – AB (manufacturer). AB was added to the media at a

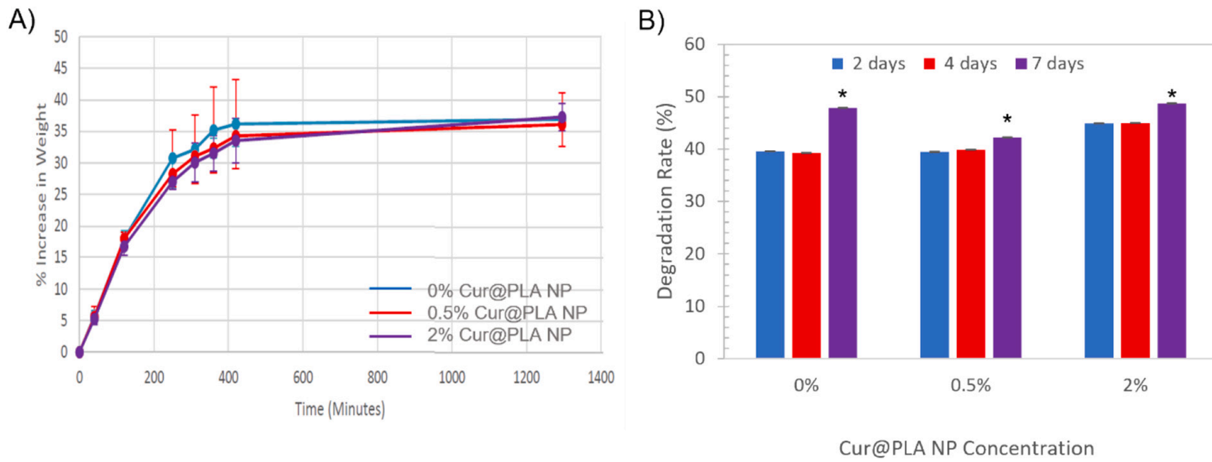

Fig. 5. Swelling ratio (A) and degradation rate (B) of prepared alginate/gelatin hydrogels with (0.5 % and 2 %) or without (0 %) Cur@PLA NPs.

Table 2
Diffusion coefficients of water through alginate/gelatin hydrogels swelling.

Sample	B	H (m)	D (m^2 s^{-1})
0 %	0.001	5×10^{-3}	0.491×10^{-11}
0.5 % Cur@PLA NPs	0.0012	5×10^{-3}	0.707×10^{-11}
2 % Cur@PLA NPs	0.0013	5×10^{-3}	0.83×10^{-11}

concentration of 10 % as specified by the manufacturer. The cells were returned to the incubator and aliquots of the media were taken after 30 min. Aliquots were measured in a 96 well-plate and fluorescence readings were performed at 540 nm and 590 nm using a SynergyMx plate reader (BioTek, EUA).

2.5. Synthesis of Cur@PLA NPs-loaded alginate-gelatin hydrogels

Cur@PLA NPs were added to PBS solutions to a final concentration of 0.5 % and 2 % (*w/v*). Then, gelatin (2.5 g) was added to the previous solution containing Cur@PLA NPs, which was stirred (600 rpm) under heat (60 °C) until gelatin was fully dissolved. After that, alginate (2.5 g) was then added to the Gelatin/Cur@PLA NPs/PBS solution to make 5 % wt% concentration. The solution was stirred at 60 °C at 600 rpm until a homogenous viscous solution was obtained. The Cur@PLA NP/polymeric solution was then centrifuged for 2 min at 2000 rpm for the removal of any air bubbles entrapped within the solution. The Cur@PLA NP/polymeric solutions were then added into a mould and allowed to crosslink overnight using a solution of $CaCl_2$ 200 mM at room temperature. Hydrogels were stored under 4 °C until further use.

2.6. Characterization of Cur@PLA NPs-loaded alginate-gelatin hydrogels

2.6.1. Hydrogel morphology and porosity

Hydrogels were prepared as described previously and freeze-dried using the Eurotherm LS 40 (Severn Science Ltd., Bristol, England). Freeze drying was carried out using the following conditions: cooling for 8 h at −30 °C, first drying for 16 h at -20 °C under 0.01 mbar and secondary drying for 2 h at 20 °C under 0.01 mBar. The freeze-dried scaffolds were then gold-coated using a gold coater (Emitech K550) prior to the SEM analysis, utilizing a Hitachi TM-1000 (Hitachi, Japan). The samples were gold coated for 1 min at 20 mA under vacuum conditions. The vacuum was set to 1×10^{-1} Pa. SEM was carried out to determine general structure and porosity using Image J software (National Institutes of Health, USA). The hydrogels were also placed on conductive copper tape and placed in the SEM.

2.6.2. Mechanical properties

Cylindrical, uniform and fully cross-linked hydrogels were needed to perform compression testing. Moulds (diameter = 13 mm, thickness = 5 mm) were used to create these hydrogels. The hydrogels were cross-linked overnight using calcium chloride. Hydrogels of different concentrations of curcumin nanoparticle solution, which included 0.1 %, 0.3 %, 0.5 %, 1 %, 2 % and 3 % nanoparticle solution were compressed in order to determine a relationship between mechanical strength and increasing concentrations of curcumin. The hydrogel was loaded between two flat plates, with the top plate moving down incrementally until the gel was fully compressed. The thickness of each hydrogel was determined using a Mitutoyo Absolute thickness gauge to determine accurate dimensions of the hydrogel. The thickness gauge provided more accurate dimensions of the hydrogels as distinct to using a Vernier caliper. Three samples of each formulation underwent compression testing. The compression testing was conducted using a Tinius Olsen H25KS materials testing machine. The parameters of the compression testing were as follows: hydrogels were compressed under a 100 N load cell at a speed rate of 0.5 mm/min. The height and thickness of each sample were recorded before testing. A force (N) *vs* displacement (mm) curve was recorded during testing, which was then converted to a stress-strain curve. Once the stress-strain curve was completed, the max stress required to break the gel was determined. Young's Modulus was also determined for each of the gels by getting the slope of the line of the stress-strain curves in the elastic region. Average max stress and Young's Modulus was determined from the three gels tested for each concentration.

2.6.3. Rheological profile

Rheological testing was conducted using a Discovery Hybrid Rheometer (DHR-2) from TA Instruments (Delaware, USA) and 25 mm parallel geometry plates. Prior to testing, the machine was calibrated for inertia and coefficient of friction and then for plate geometry. Viscosity was investigated as a function of shear rate as it increased from 1 to 1000 1/s. Loss modulus and storage modulus were obtained using a strain sweep test ranging from 0.0125 % to 100 % strain and angular frequency of 5.0 rad/s. Both tests were conducted at 25 °C.

2.6.4. Swelling profile

Swelling testing was carried out on the hydrogels of different concentrations of curcumin nanoparticle solution. 3 samples of each concentration were used in the testing. The hydrogels were dried overnight in a vacuum oven at 50 °C at 900 psi to remove any water in the gels. The dry weight of the hydrogels was then measured and weighed. The gels were then submerged in PBS and placed in a water bath at 37 °C. The gels were then weighed at different time points to determine the swell

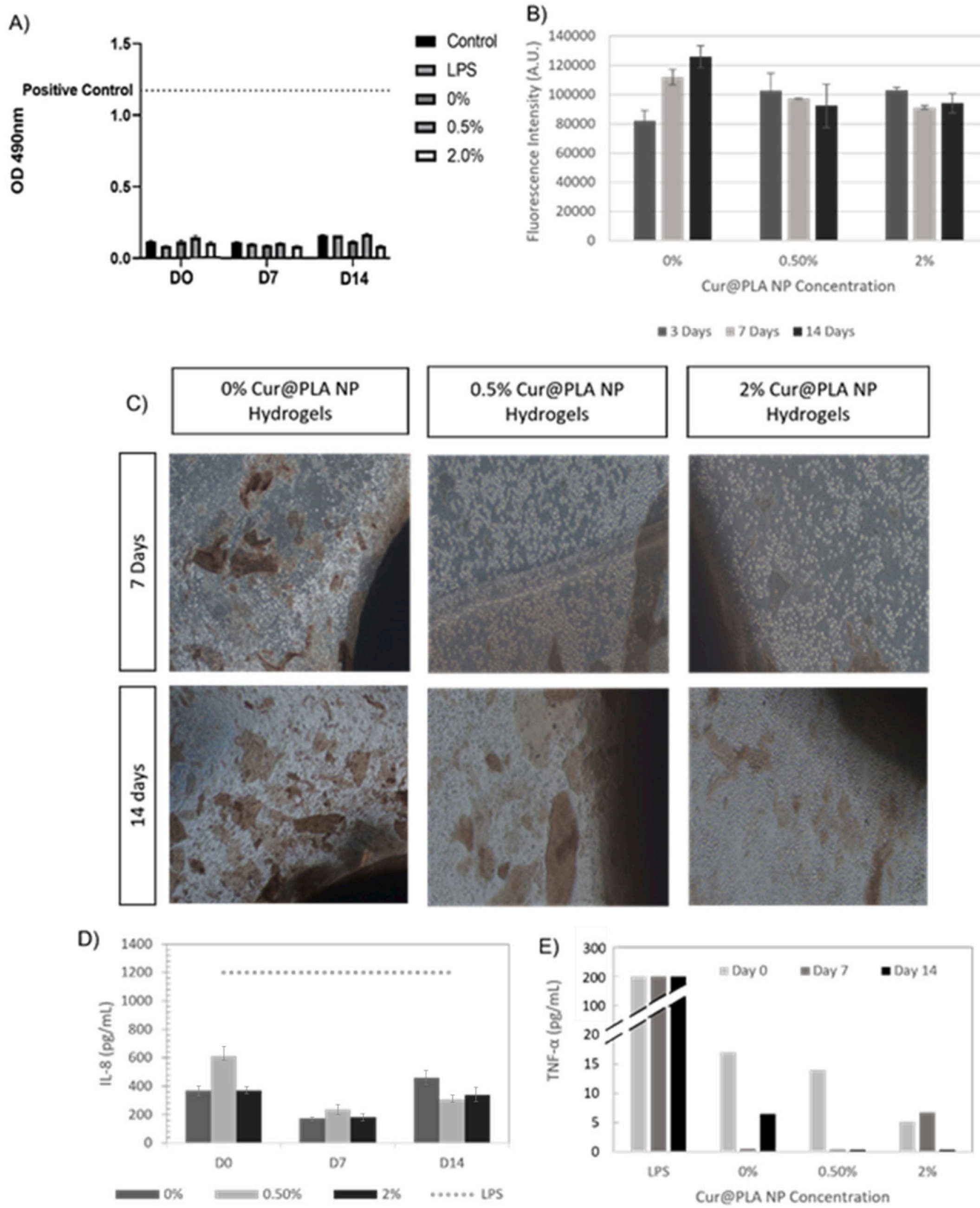

Fig. 6. THP-1 cytocompatibility of Cur@PLA NP-loaded alginate/gelatin hydrogels using LDH assay (A) and Alamar Blue (B). Optical micrographs of THP-1 incubated with Cur@PLA NP-loaded alginate/gelatin hydrogels for 7 and 14 days (C). Pro-inflammatory cytokines production profile of IL-8 (D) and TNF-α (E) when THP-1 cells are exposed to Cur@PLA NP-loaded alginate/gelatin hydrogels.

ratio of the gels. The time points chosen were 15mins, 30mins, 1 h, 2 h, 3 h, 22 h and 24 h. Three samples of each concentration were used for testing purposes. The swell ratio was determined using the following formula:

$$SR\ (\%) = \frac{W_S - W_D}{W_D} \times 100$$

where W_S is the swelled weight of the hydrogel, W_D is the dry weight and SR is the swelling ratio.

2.6.5. *Structural analysis*

Hydrogels were prepared and freeze-dried for 24 h, as described previously, before the chemical characterization of the hydrogels were conducted. All spectra were recorded on a Perkin Elmer spectrum 100 FT-IR spectrometer operating in the Attenuated Total Reflectance (ATR) mode (Perkin Elmer, USA). Each FTIR spectrum was scanned 12 times with a resolution of 4 cm^{-1}.

2.6.6. *Degradation profile*

A degradation test was conducted by submerging the hydrogels in a PBS solution at 37 °C for various time periods for up to one week. The wet weight of the hydrogels was weighed at each time point from the PBS and then freeze-dried. The freeze-dried samples were also weighed. The degradation rate of the freeze-dried samples was recorded. The extent of degradation was determined by weight loss of the samples as follows:

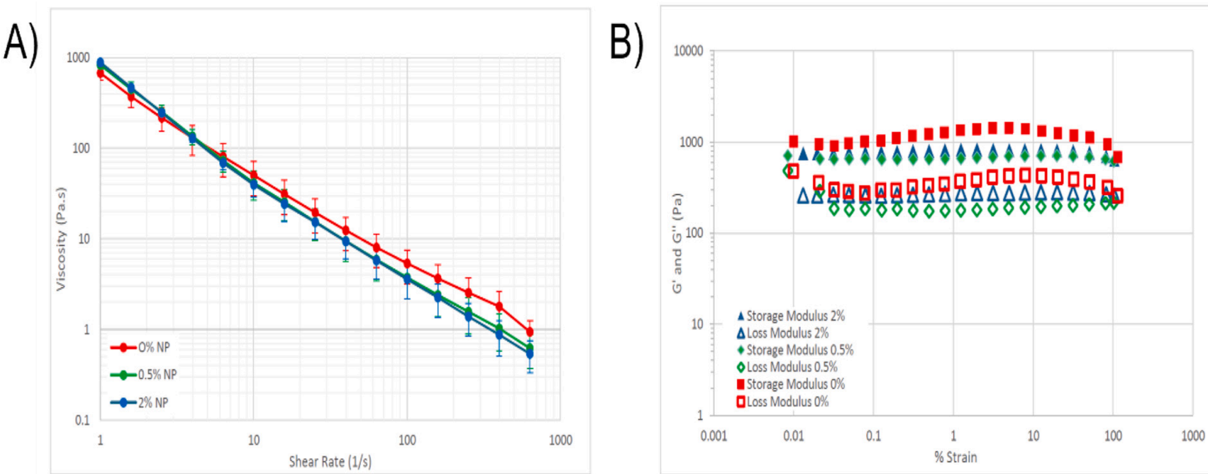

Fig. 7. Shear thinning (A) and viscoelastic (B) properties of 0 %, 0.5 % and 2 % Cur@PLA NP-loaded alginate/gelatin solutions for 3D printing.

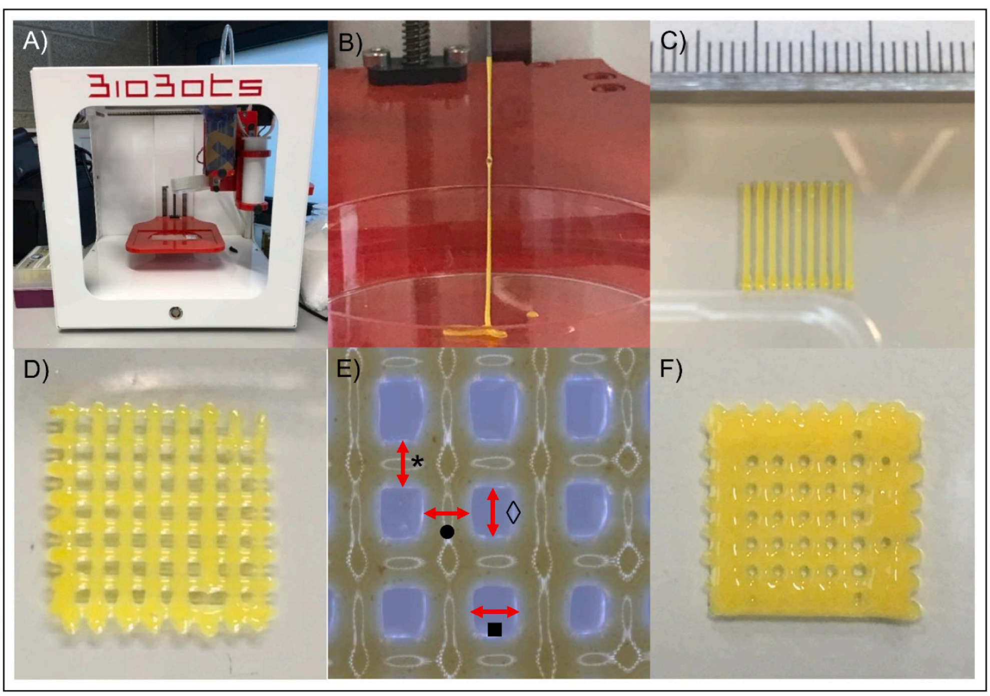

Fig. 8. 3D printing Cur@PLA NP-loaded hydrogels. A) BioBots 3D printer. B) Extruded Cur@PLA NPs-loaded alginate/gelatin filament at correct printing pressure. C) Single layer printed scaffold D) Double layer printed scaffold E) Close up image of double layer printed scaffold. Dimensions shown in red arrows are as follows: * 0.532 mm; ● 0.607 mm; ◊ 0.9593 mm; ▪ 0.540 mm. F) 3D printed four-layered scaffold.

$$D(\%) = \frac{W_I - W_T}{W_I}$$

where D is the degradation rate, W_I is the initial weight of the sample, and W_T is the weight of the sample at the specified time point.

2.6.7. *In vitro cytocompatibility of Cur@PLA NP-loaded alginate/gelatin hydrogels*

THP-1 cells were assessed for viability using LDH activity assay. Briefly, after cells were incubated with various groups of Cur@PLA NP-loaded hydrogels (0 %, 0.5 % and 2 % *w/v*) for 1 day, 7 days and 14 days. The supernatant was collected after each timepoint and assessed for LDH activity. The percentage of LDH released from THP-1 cells to the culture medium was quantified by measuring absorbance at 490 nm using a SynergyMx plate reader (BioTek, EUA) as described by the manufacturer.

Alginate/gelatin hydrogels doped with various concentrations of Cur@PLA NPs were cultured with THP-1 cells in order to analyse whether the curcumin present on the hydrogels displayed any anti-inflammatory property. For the immune activation analysis, THP-1 cells at a density of 2×10^5 cell/mL were seeded onto Cur@PLA NP-loaded alginate/gelatin hydrogels (0 %, 0.5 % and 2 % *w/v*) for 1 day, 7 days and 14 days. After each incubation period, supernatant was collected by centrifugation and analysed for the production of TNF-α and IL-8 cytokines, as described by the ELISA kit manufacturer.

2.7. *3D printing of Cur@PLA NP-loaded alginate/gelatin hydrogels*

The 2 % Cur@PLA NPs-loaded alginate/gelatin hydrogel was tested as a possible bioink for a 3D printed hydrogel scaffold. The prepared solution was loaded into a syringe for printing that had the plunger removed to allow the air pressure from the compressor to extrude the bioink using a 3D extrusion printer (Allevi BioBot Inc., Philadelphia, USA). In order to determine the correct pressure for printing, a low starting pressure was initially used (<5 PSI) and this was incrementally increased until a steady stream of filament could be extruded. The designed scaffolds used a 0.2 mm diameter design for each line. The slicing used in Repetier Host was 0.2 mm, with a print speed defined as 3 mm/s. The temperature setting was kept constant at 25 °C.

2.8. Statistical analysis

Data are presented as mean ± standard deviation (s.d.) and analysed using one-way analysis of variance (ANOVA) followed by post-hoc Tukey's HSD test. *P*-values <0.05 (*) were considered significant.

3. Results and discussion

3.1. Cur@PLA NPs synthesis and characterization

NPs were produced using an oil in water, solvent evaporation method. Single emulsion solvent evaporation method is the most efficient way to encapsulate hydrophobic compounds [23]. The most important step in creating the NPs is the formation of an oil in water emulsion, consisting of an organic phase and an aqueous phase which can be seen in Fig. 1A. The organic phase, which consists of curcumin and PLA dissolved in DCM, and am aqueous phase containing SDS (surfactant) dissolved in deionized water. When an emulsion is created (in this case using sonication) the surfactant reduces the surface tension between the two phases and prevent droplet coalescence (shown in Fig. 1B) [24]. This emulsion creates nanodroplets that once the organic solvent is removed by freeze drying leaves particles with nanometre size, as show in Fig. 1C. The yield of 0.02378 g/mL of Cur@PLA NPs was calculated after freeze drying.

The Cur@PLA NPs were then visualized under SEM, as seen in Fig. 1D. Cur@PLA NPs morphology is spherical with a smooth surface. The size of the NPs was measured, and they range between 50 and 250 nm with an average size of 160 nm. The size of the Cur@PLA NPs is consistent with other studies. For example, the average size of curcumin/PLA, curcumin/PLA/PEG and curcumin-PLGA NPs has been reported as 300 nm, 150 nm, and 200 nm, respectively [25–27]. Moreover, curcumin NPs also show approximately a 5.5-fold increase in bioavailability compared to that of crude curcumin [27].

In order to assess the safety and biocompatibility of the novel Cur@PLA NPs, NHI 3 T3 fibroblasts were incubated with various ascending concentrations of Cur@PLA NPs solutions (shown in Fig. 1E). Results showed that independently of Cur@PLA NP concentration, cell proliferation is not impaired, in agreement with previous studies showing curcumin safety even at high doses [13]. However, although not significantly different from control, higher concentrations of Cur@PLA NPs show a tendency to slow fibroblast proliferation.

3.2. Bioink development and characterization

After the synthesis of Cur@PLA NPs, they were incorporated into 5 % alginate and 5 % gelatin solutions. Three formulations were prepared according to Cur@PLA NP concentration: control group (0 % Cur@PLA NPs) did not contain any Cur@PLA NP and was synthesised using alginate and gelatin alone; 0.5 % Cur@PLA NPs; and 2 % Cur@PLA NPs. After centrifuging the resulting solutions, they were placed in specially designed metallic moulds (Fig. 2A), to create uniform, cylindrical shaped hydrogels upon ionic crosslinking using a 200 mM $CaCl_2$ solution (Fig. 2B). Hydrogels were then freeze dried for future testing, shown in Fig. 2C.

The morphology of the alginate/gelatin hydrogels with or without the incorporation of Cur@PLA NPs was investigated using a SEM. Fig. 3 shows the surface and cross-sectional morphologies of the various hydrogel formulations. The 2 % and 0.5 % Cur@PLA NP-loaded hydrogels did display a porous structure, while the control group containing alginate/gelatin alone (0 % Cur@PLA NPs) did not. Porous size was measured using Image J, and results show that 0.5 % Cur@PLA NP-loaded hydrogels have an average pore size of 28 μm, and 2 % Cur@PLA NP-loaded hydrogels have an average pore size of 19 μm.

The FTIR spectra of Cur@PLA NP-loaded alginate/gelatin hydrogels are shown in Fig. 3.The band located at 1030 cm^{-1}–1085 cm^{-1}, is related to C—C and C—O stretching in the alginate crosslinked structure [28]. The presence of the bands at 1601 and 1412 cm^{-1} are attributed to asymmetric and symmetric stretching vibrations of the the-COO- carboxylic groups in alginate. In addition the samples with Cur@PLA NP show a more intense band located at 1550 cm^{-1} which is attributed to the stretching of the carbonyl groups of curcumin [29]. Moreover, the strong absorption of the samples in the carbonyl region is also attributed to the amide I band corresponding to the C—O and C—N stretching of the gelatin. In addition, the presence of geleatin is evidenced with the small shoulder at 1550 cm^{-1} represents the amide II band while the amide III is visible at 1238 cm^{-1} representing the C—N stretching and N—H bending. All hydrogels display the characteristic band of alginate at 3284 cm^{-1} for O—H stretching.

Compressive stress *vs* starin curves for freshly crosslinked hydrogel samples are shown in Fig. 4A. The Young's Moduli are shown in Fig. 4B. Hydrogels in freeze-dried and swollen states had their Young's moduli calculated when strain was smaller than 6 % (linear region defined by Hooke's law). The Young's Moduli of freeze-dried samples ranged between 3 and 3.5 kPa, while the Young's Moduli of swollen hydrogel samples were below 0.5 kPa.

The concentration of nanoparticle concentration does not seem to impact (not significantly) the compressive strength of the hydrogels.

Swelling and degradation tests are shown in Fig. 5A and B, respectively. Gels are swollen to their equilibrium within the first 6 h of incubation with all hydrogels reaching their swelling plateau. There is no evidence of correlation between NP concentration and swelling ratio.

Most of the degradation (approximately 40 % degradation) of the hydrogels occurred inside the first two days, with little to no degradation occurring between 4 and 7 days. Pan, Song, Cao and Wang conducted a degradation study on alginate-gelatin based hydrogels and had a similar degradation rate of approximately 40 % for their $CaCl_2$ cross-linked gels [28]. There is no evidence between degradation % and curcumin nanoparticle concentration at low concentrations of NP. The most likely cause of the degradation of the hydrogels is due to the alginate, as ionically cross-linked alginate are shown to leach Ca^{2+} ions and increase gel dissociation [30]. The reaction of alginate and PBS most likely caused a fast degradation rate, as PBS has a high salt content and it has been shown to cause the collapse of the alginate network [31].

Diffusion coefficients for water lie in the range of 0.491×10^{-11} m^2 s^{-1} and 0.83×10^{-11} m^2 s^{-1}, Table 2. These figures are in agreement with the literature [32].

3.2.1. Biological characterization of Cur@PLA NP-loaded alginate/gelatin hydrogels

The evaluation of cell viability was performed using LDH and Alamar Blue assays on THP-1 cells incubated with the Cur@PLA NP-loaded alginate/gelatin hydrogels (shown in Fig. 6A and B, respectively). The visual interaction of cells and hydrogels is shown in Fig. 6C. The level of LDH release is considered relatively low across all time points and demonstrates that cell plasma membrane maintains intact. The hydrogels did not cause excessive cell death or apoptosis as the LDH produced by the hydrogels is much lower than the positive control. This would suggest that the hydrogels synthesised have neglectable negative effect on cell viability which corroborates the assumption that alginate, gelatin and Cur@PLA NPs are cytocompatible. Moreover, the cellular metabolic activity is not compromised when incubated with the hydrogels containing Cur@PLA NPs.

The immunomodulatory response of the Cur@PLA NP-loaded alginate/gelatin hydrogels on THP-1 cells is shown in Fig. 6D and E. Quantification of pro-inflammatory cytokines (TNF-α and IL-8) was evaluated using ELISA test in order to determine whether Cur@PLA NPs can inhibit or suppress the regulation of these cytokines. Curcumin has already been shown to exhibit an anti-inflammatory response on human chondrocytes when tested *in vitro* [33]. While the ability to down-regulate TNF-α and IL-8 is mediated by the inhibitory effects on signal pathways such as NF-kB and MApks [34,35].

Results in Fig. 6D show that all alginate/gelatin hydrogels, independently of Cur@PLA NP concentration, have similar IL-8 production profiles. THP-1 cells are not over induced to produce IL-8 by the hydrogels in comparison to well know inducers such as LPS. However, TNF-α production decreases overtime to negligible amounts for both 0.5 % and 2 % Cur@PLA NP-loaded hydrogels (Fig. 6E). 0 % Cur@PLA NP hydrogels still show high levels of TNF-α production. The result strongly suggests that curcumin is responsible for the downregulation of TNF-α production. THP-1 cells appear to better tolerate the alginate/gelatin hydrogels by its decreased production of TNF- α when incubated with higher amounts of Cur@PLA NPs, as shown in 2 % Cur@PLA NP-loaded hydrogels.

3.3. 3D printing Cur@PLA NP-loaded alginate/gelatin bioinks

Fig. 7A shows the effect of increasing shear rate on viscosity. The 0.5 % and 2 % Cur@PLA NP-loaded samples behave similarly under increasing shear rate, while control samples (0 % Cur@PLA NP) appear to be less sensitive to shear.

In order to determine the storage modulus (G') and loss modulus (G") a strain sweep test was performed (Fig. 7B), where G' represents the elastic component and G" represents the viscous component of the formulation. Ideally a bioink should have a higher storage modulus than loss modulus, as this allows the printed material to maintain its shape and prevent filaments deforming after extrusion [36]. In Fig. 7B, the storage modulus remained higher than the loss modulus across all samples within the tested strain range.

The 2 % Cur@PLA NP-loaded 5 % alginate/5 % gelatin was selected as a candidate bioink and successfully printed into a grid shape, as shown in Fig. 8, with a double layer showing excellent shape retention. The width of the printed lines, shown in Fig. 8E, is 0.5 mm.

4. Conclusion

Curcumin encapsulation was successful when using PLA as the polymeric encapsulant in an oil in water emulsion, solvent evaporation method. The incorporation of the Cur@PLA NPs in alginate-gelatin hydrogels increased the compressive strength and mechanical performance of the hydrogels. However, Cur@PLA NPs did not influence the swellability and degradation profiles of the hydrogels. Cur@PLA NPs-loaded alginate/gelatin hydrogels have also shown a positive effect on cell growth of fibroblast and preserved the viability of monocytes. Hydrogels released Cur@PLA NPs to inhibit TNF-α cytokine production by monocytes. Of the various formulations used to develop the Cur@-PLA NP-loaded hydrogels, the incorporation of 2 % Cur@PLA NPs shows optimal performance. For this reason, 2 % Cur@PLA NP-loaded hydrogels were assessed as a novel bioink for 3D printing. It was successfully printed into a 4-layer scaffold. However, the 2-layered structure showed better shape retention. The bioink has been used to create simple three-dimensional structures. Further studies should be performed to optimize and tailor these bioinks in terms of mechanical performance for future implantation constructs for IVDD.

CRediT authorship contribution statement

Fernanda Zamboni: Funding acquisition, Investigation, Methodology, Writing – original draft, Writing – review & editing. **Guang Ren:** Investigation, Methodology, Writing – original draft, Writing – review & editing. **Mario Culebras:** Formal analysis, Investigation, Methodology, Writing – original draft, Writing – review & editing. **John O'Driscoll:** Data curation, Formal analysis, Investigation, Methodology, Writing – original draft. **Jack O'Dwyer:** Data curation, Formal analysis, Investigation, Methodology, Writing – original draft. **Elizabeth J. Ryan:** Formal analysis, Investigation, Methodology, Writing – original draft. **Maurice N. Collins:** Formal analysis, Funding acquisition, Investigation, Methodology, Project administration, Resources, Software, Supervision, Writing – original draft, Writing – review & editing.

Declaration of competing interest

The authors declare that they have no known competing financial interests or personal relationships that could have appeared to influence the work reported in this paper.

Data availability

Data will be made available on request.

Acknowledgements

The authors would like to thank the funding provided by the Irish Research Council through the IRC Postdoctoral Fellowship (GOIPG/2021/75).

Appendix A. Supplementary data

Supplementary data to this article can be found online at https://doi.org/10.1016/j.ijbiomac.2022.09.014.

References

[1] T. Oichi, et al., Pathomechanism of intervertebral disc degeneration, JOR Spine 3 (1) (2020), e1076.
[2] J.N. Katz, Lumbar disc disorders and low-back pain: socioeconomic factors and consequences, JBJS 88 (suppl_2) (2006).
[3] Y. Wang, et al., The role of IL-1β and TNF-α in intervertebral disc degeneration, Biomed. Pharmacother. 131 (2020), 110660.
[4] E.J. Novais, et al., Long-term treatment with senolytic drugs Dasatinib and Quercetin ameliorates age-dependent intervertebral disc degeneration in mice, Nat. Commun. 12 (1) (2021) 5213.
[5] P. Sampara, et al., Understanding the molecular biology of intervertebral disc degeneration and potential gene therapy strategies for regeneration: a review, Gene Ther. 25 (2) (2018) 67–82.
[6] M. Loibl, et al., Controversies in regenerative medicine: should intervertebral disc degeneration be treated with mesenchymal stem cells? JOR Spine 2 (1) (2019), e1043.
[7] C.K. Lee, et al., Advances in tissue engineering for disc repair, Appl. Sci. 11 (4) (2021) 1919.
[8] S.K. Mirza, A.A. White 3rd, Anatomy of intervertebral disc and pathophysiology of herniated disc disease, J. Clin. Laser Med. Surg. 13 (3) (1995) 131–142.
[9] L. Xiao, et al., Curcumin prevents tension-induced endplate cartilage degeneration by enhancing autophagy, Life Sci. 258 (2020), 118213.
[10] H. Cherif, et al., Curcumin and o-vanillin exhibit evidence of senolytic activity in human IVD cells in vitro, J. Clin. Med. 8 (4) (2019) 433.
[11] V. Rolfe, et al., Turmeric/curcumin and health outcomes: a meta-review of systematic reviews, Eur.J.Integr.Med. 40 (2020), 101252.
[12] J. Sharifi-Rad, et al., Turmeric and its major compound curcumin on health: bioactive effects and safety profiles for food, pharmaceutical, biotechnological and medicinal applications, Front. Pharmacol. 11 (2020).
[13] C.D. Lao, et al., Dose escalation of a curcuminoid formulation, BMC Complement. Altern. Med. 6 (2006) 10.
[14] M.E. Abd El-Hack, et al., Curcumin, the active substance of turmeric: its effects on health and ways to improve its bioavailability, J. Sci. Food Agric. 101 (14) (2021) 5747–5762.
[15] S.C. Gupta, S. Patchva, B.B. Aggarwal, Therapeutic roles of curcumin: lessons learned from clinical trials, AAPS J. 15 (1) (2013) 195–218.
[16] A. Umerska, et al., Polymeric nanoparticles for increasing oral bioavailability of curcumin, Antioxidants 7 (4) (2018) 46.
[17] Y.-S. Fu, et al., Pharmacological properties and underlying mechanisms of curcumin and prospects in medicinal potential, Biomed. Pharmacother. 141 (2021), 111888.

[18] T.C. Schmitz, et al., Characterization of biomaterials intended for use in the nucleus pulposus of degenerated intervertebral discs, Acta Biomater. 114 (2020) 1–15.
[19] G. Tang, et al., Advances of naturally derived and synthetic hydrogels for intervertebral disk regeneration, Front.Bioeng.Biotechnol. 8 (2020).
[20] A. Krouwels, et al., Focal adhesion signaling affects regeneration by human nucleus pulposus cells in collagen- but not carbohydrate-based hydrogels, Acta Biomater. 66 (2018) 238–247.
[21] P. Xu, et al., Stiffness of photocrosslinkable gelatin hydrogel influences nucleus pulposus cell properties invitro, J. Cell. Mol. Med. 25 (2) (2021) 880–891.
[22] B. Sarker, et al., Macromolecular interactions in alginate–gelatin hydrogels regulate the behavior of human fibroblasts, J. Bioact. Compat. Polym. 32 (3) (2017) 309–324.
[23] A. Mathew, et al., Curcumin loaded-PLGA nanoparticles conjugated with Tet-1 peptide for potential use in Alzheimer's disease, PLOS ONE 7 (3) (2012), e32616.
[24] M. Jaiswal, R. Dudhe, P.K. Sharma, Nanoemulsion: an advanced mode of drug delivery system, 3Biotech 5 (2) (2015) 123–127.
[25] H. Rachmawati, et al., Curcumin-loaded PLA nanoparticles: formulation and physical evaluation, Sci. Pharm. 84 (1) (2016) 191–202.
[26] H. Liang, J.M. Friedman, P. Nacharaju, Fabrication of biodegradable PEG-PLA nanospheres for solubility, stabilization, and delivery of curcumin, Artif. Cells Nanomed. Biotechnol. 45 (2) (2017) 297–304.
[27] X. Xie, et al., PLGA nanoparticles improve the oral bioavailability of curcumin in rats: characterizations and mechanisms, J. Agric. Food Chem. 59 (17) (2011) 9280–9289.
[28] T. Pan, et al., 3D bioplotting of gelatin/alginate scaffolds for tissue engineering: influence of crosslinking degree and pore architecture on physicochemical properties, J.Mater.Sci.Technol. 32 (9) (2016) 889–900.
[29] R.S. P, et al., Preparation, characterization and biological evaluation of curcumin loaded alginate aldehyde-gelatin nanogels, Mater. Sci. Eng. C Mater. Biol. Appl. 68 (2016) 251–257.
[30] K.Y. Lee, D.J. Mooney, Alginate: properties and biomedical applications, Prog. Polym. Sci. 37 (1) (2012) 106–126.
[31] S.K. Bajpai, S. Sharma, Investigation of swelling/degradation behaviour of alginate beads crosslinked with Ca2+ and Ba2+ ions, React. Funct. Polym. 59 (2) (2004) 129–140.
[32] A.F. Stockwell, S.S. Davis, S.E. Walker, In vitro evaluation of alginate gel systems as sustained release drug delivery systems, J. Control. Release 3 (1) (1986) 167–175.
[33] B.S. Qazi, K. Tang, A. Qazi, Recent advances in underlying pathologies provide insight into interleukin-8 expression-mediated inflammation and angiogenesis, Int. J. Inflamm. 2011 (2011), 908468.
[34] J.-W. Cho, K.-S. Lee, C.-W. Kim, Curcumin attenuates the expression of IL-1β, IL-6, and TNF-α as well as cyclin E in TNF-α-treated HaCaT cells; NF-κB and MAPKs as potential upstream targets, Int. J. Mol. Med. 19 (3) (2007) 469–474.
[35] Y. Zhang, Y. Zeng, Curcumin reduces inflammation in knee osteoarthritis rats through blocking TLR4 /MyD88/NF-κB signal pathway, Drug Dev. Res. 80 (3) (2019) 353–359.
[36] Front-matterA.M. Asiri Inamuddin, A. Mohammad (Eds.), Applications of Nanocomposite Materials in Drug Delivery, Woodhead Publishing, 2018, pp. i–iii.